VISUAL SERVOING APPROACH TO COLLISION AVOIDANCE FOR AIRCRAFT

Aaron Mcfadyen*,, Luis Mejias*,** , Peter Corke***
***Queensland University of Technology, ****Australian Research Centre for Aerospace Automation**
aaron.mcfadyen@qut.deu.au; luis.mejias@qut.edu.au; p.corke@qut.edu.au

Keywords: *Collision Avoidance, Visual Servoing, Sense and Avoid, Aerial Robotics*

Abstract

This paper presents a reactive Sense and Avoid approach using spherical image-based visual servoing. Avoidance of point targets in the lateral or vertical plane is achieved without requiring an estimate of range. Simulated results for static and dynamic targets are provided using a realistic model of a small fixed wing unmanned aircraft.

1 Introduction

Unmanned aircraft (UAS) have been identified as a potential solution to a broad range of civilian tasks, yet a number of regulatory and technological barriers must be overcome first [1] [2] [3]. The most significant technological issue restricting the integration of autonomous unmanned aircraft into the national airspace is their inability to independently detect and avoid unplanned hazards during flight. This is more commonly referred to as See & Avoid in conventionally-piloted aircraft and can be considered a form of decentralized, short term collision avoidance of both static and dynamic targets. According to international regulatory bodies[1], any automated See & Avoid[2] system needs to demonstrate the equivalent level of safety (ELOS) to manned aircraft so a natural choice for the detect function is the use of computer vision [4]. Recent work has been focused on the detection and tracking of aerial targets from monocular vision [5] [6] [7], as this would allow even the smallest UAS to have such capability. Computer vision is not without its drawbacks, with recent technology helping to overcome these. Of significance are developments in spherical imaging from wide angle lenses [8] [9] [10] and image processing techniques [11]. These developments may relax the harsh constraints on camera field of view[3] and allow earlier target detection in a broader range of environmental conditions. The next challenge is to decide how to use the visual information and act in a timely manner to avoid collision.

A large number of conflict resolution approaches have been proposed [12] but most cannot be used with a visual sensor. This is due to the limited amount of information that can be obtained from monocular cameras and time allowed to resolve the conflict [13] [14] [15]. Approaches based on range or bearing rate [16] may be optimistic according to recent studies [17] [18].

Recently image-based visual servoing (IBVS) has been used to control fixed wing aircraft but often require multiple image features for a complete control solution [19]. If applied to collision avoidance, IBVS would provide a reactive solution that allows feedback control to be derived directly from the image space without the need for target state estimation [20]. In [21]

[1]Federal Aviation Administration AIM chapter 8 (USA), Civil Aviation Safety Authority (Australia) and EuroControl (Europe)

[2]Often referred to as Sense & Avoid for UAS

[3]Objects positioned greater than 90° azimuth angle from camera optical axis remain visible using spherical imaging surfaces

and [22], a vision based control approach is used to avoid large and near targets and depends on extracting a qualative range estimate to drive a proportional controller for pitch and roll. In [23] and [24], collision avoidance of a cylindrical target is achieved by holding the cylinder edge at a fixed angle in the image. The approach is 2 dimensional, providing lateral avoidance only, and does not consider the ego motion from the camera. Although range is not required for control, it is used to ensure the aircraft does not spiral back toward the target. This spiral like motion has been observed in insects [25] and has been exploited by [26] to derive a similar collision avoidance controller. The vertical velocity and yaw rate are used to control altitude and lateral position of a quad rotor but requires a course estimate of range for control. The stopping criteria is range independent however.

Based on previous works [6] [23] [26], we approach the conflict resolution problem as a spherical image-based visual servoing task using single point features. We derive a controller for yaw and pitch that attempts to hold a fixed azimuth or elevation angle without a range estimate. This allows flexibility in the autopilot configuration and avoidance direction. We exploit the wide field of view provided by spherical cameras and design a stopping criteria based on the rules of the air [27] and the expected requirements on Sense and Avoid functionality.

In section 2 we describe aircraft detection in the context of spherical imaging. We derive the guidance and control approach in section 3 and show the alignment of the visual control architecture with the generic Detect, Decide and Act framework for Sense and Avoid. Section 4 presents preliminary results for the avoidance of static and constant velocity targets using a full non-linear aircraft model of a small fixed wing UAS.

2 Detection

A potential collision target appears as a small, slow moving image point occupying only a few pixels until it rapidly expands when very close. At this time it may be to late to avoid collision, so recent studies have focused on the detection and tracking of pixel size targets from aerial platforms [7] [11]. Flight test results using perspective imaging devices indicate initial detection of GA aircraft up to 3000m away and small UAS up to 900m [5]. Therefore, the time allocated for collision avoidance is limited. Maneuvering to recover range is not only unreliable but may potentially worsen the situation [18]. Additionally, the target may exit the camera field of view when using perspective imaging devices. Although under development, spherical cameras offer a 4π steradians field of view and allow for target visibility regardless of its relative position [9] and own ship orientation. The unified imaging model of [10] can be used to map a point on a planar imaging device to a section of a spherical imaging surface. Multiple perspective camera could be used to then create an approximation to a sphere [8]. The mapping from perspective to spherical cameras is shown in figure 1 and 2 with details provided in [10].

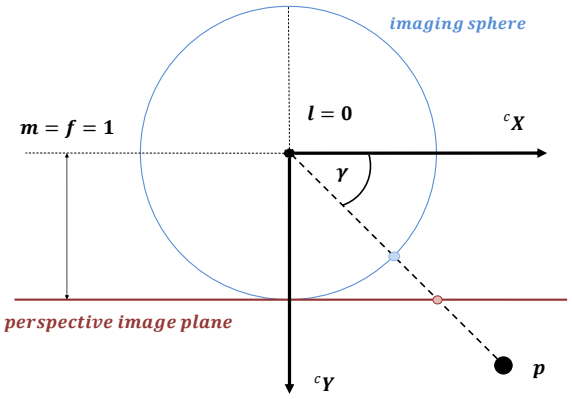

Fig. 1 Azimuth estimation from perspective imaging

A single point feature can then be expressed using two angles, azimuth γ and colatitude σ. If the camera is attached to the body, it inherits the aircraft dynamics and the angles change not only with aircraft position, but aircraft attitude. The geometry is shown in figure 3 with the camera aligned to the body frame and positioned at its center of mass. This is not the only choice for camera orientation and the azimuth and colati-

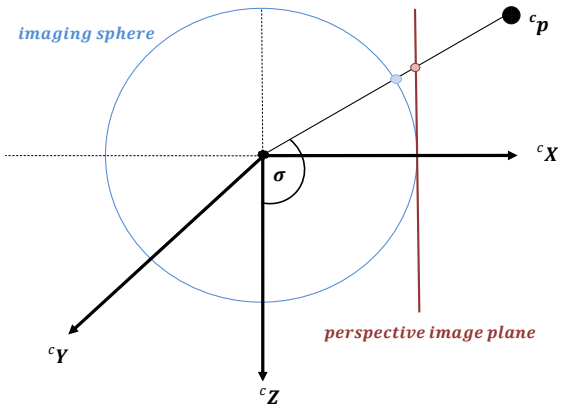

Fig. 2 Colatitude estimation from perspective imaging

tude angle would change accordingly.

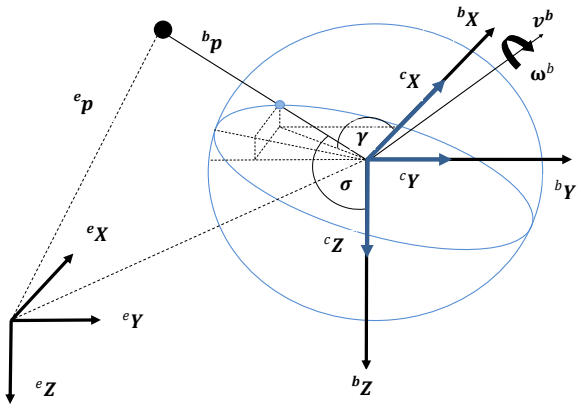

Fig. 3 Collision geometry. The spherical camera is attached to the aircraft free to move in inertial space. The relationship between the target and the inertial, body and camera frames is shown

3 Guidance & Control

We propose the control architecture depicted in 4. We assume that target detection has been addressed and the guidance and control loops have knowledge of the target position in the image. A high level controller determines which guidance source to use; visual control for short term collision avoidance and way point navigation otherwise. If the target appears in the image, we initially consider it a threat based on the expected detection distance and the approximate time before collision when using visual sensors [13] [14] [15].

From figure 3, it is clear that provided we derotate the aircraft, azimuth and colatitude angle can be used to measure relative bearing and elevation. Adjusting these angles could then control lateral and vertical position of the aircraft. If we

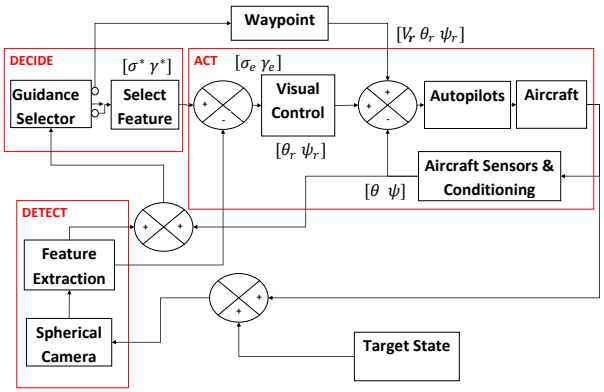

Fig. 4 Aircraft guidance & control architecture for collision avoidance

hold a static target at a fixed colatitude and azimuth angle in straight and level flight, we will spiral around the target [25]. If the magnitude of the azimuth angle is greater than 90° we will spiral outward and away from the target and therefore avoid collision. The colatitude angle determines the vertical position of the spiral trajectory. If less than 90° we spiral below the target and above otherwise [25]. Depending on where the target is initially detected, we choose our desired azimuth angle in the image such that its magnitude is greater than 90° and colatitude angle other than 90°.

So if the object is detected to the right and above the image center, we set $\gamma^* = 110°$ and $\sigma^* = 135°$. We would choose $\gamma^* = -110°$ and $\sigma^* = 45°$ if the target was initially detected below and to the left of the aircraft. This ensures the image features do not cross the lateral or vertical centerlines of the image. Additionally, less control effort would be required to achieve the desired image feature positions. The azimuth values have been chosen based on expected Sense and Avoid field of view requirements [2] [3]. These can be visualized using figure 5, which shows a section of the spherical imaging surface. We use color to highlight the regions in which po-

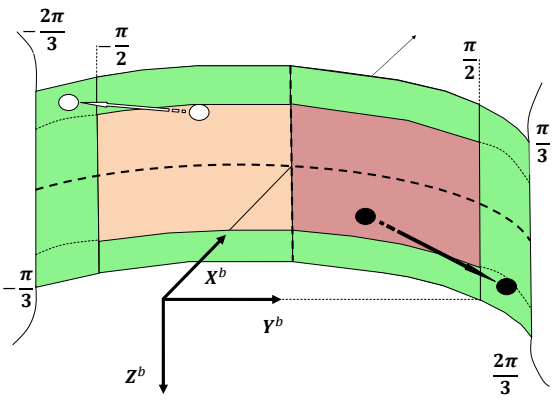

Fig. 5 Spherical section and importance of target image position. The green zones indicate safe regions and the red and orange potentially dangerous regions.

tentially dangerous conditions exist. The left side of the image is considered less hazardous based on [27].

Once the target has been moved passed an azimuth of 90° left or right in the de-rotated image, it is no longer the responsibility of the own ship to avoid the target. A simple criteria based on aircraft heading and pitch angle is used to terminate the visual control during an encounter. Once the current heading angle has decreased beyond the absolute value of the heading at initial detection, the lateral avoidance is stopped. The same logic is applied to the pitch angle for vertical avoidance. This ensures the aircraft does not spiral back toward the target in either dimension. A similar stopping criteria was successfully used in [26] for quad rotor control.

3.1 Visual Controller

We use well established image based visual servoing techniques to derive a controller capable of moving the image features to the desired position with rotational velocity only [20]. The classical image based control equation is given in (1)

$$[\mathbf{v}\ \boldsymbol{\omega}] = -\lambda \hat{\mathbf{L}}_s^{+}\mathbf{e} \tag{1}$$

where λ is a constant gain term and $\hat{\mathbf{L}}_s^{+}$ is the pseudoinverse of the image Jacobian defined by (3) and derived in [29]. The image feature error $\mathbf{e}$ is obtained by differencing the current image feature vector from the constant desired image feature vector $\mathbf{s}^*$. To control the rotational degrees of freedom, we adjust the control law by partitioning the image Jacobian [20] and arrive at (2),

$$\boldsymbol{\omega} = \hat{\mathbf{L}}_{\omega}^{+}[-\lambda\mathbf{e} - \frac{1}{R}\mathbf{L}_t\mathbf{v}] \tag{2}$$

where $\mathbf{L}_t$ consists of the Jacobian columns related to the translational velocity. $\mathbf{v}$ is the vector of translational velocities and $\boldsymbol{\omega}$ is the angular velocity vector consisting of roll, pitch and yaw rate. Using the control defined by (2), we analyze the motion in the context of aircraft capability and collision avoidance performance. We select the desired image features to be $\mathbf{s}^* = [135°\ 110°]$ and assume a constant aircraft velocity of 58kts. A static target is positioned directly in front of the camera at 500m away in the x direction. In figure

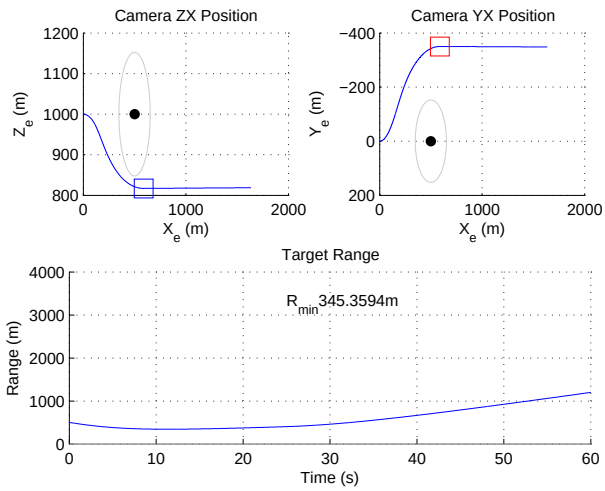

Fig. 6 Position & range to target using Roll, Pitch and Yaw control.

6, the camera position and range to a static target is shown, with the minimum safe miss distance (500 feet) indicated by the grey circle. The black point indicates target position, whilst the blue and red squares show the point at which the vertical and lateral stopping criteria were met. The trajectory is smooth and follows a spiral like pattern with initial displacements in the lateral and vertical directions in favor of collision avoidance. The stopping criteria has ensured successful collision avoidance, and the camera has not spiraled toward the target in either the vertical or lateral planes. A smooth control has also ensured the

$$L_s = \begin{bmatrix} \frac{-\cos(\sigma)\cos(\gamma)}{R} & \frac{-\cos(\sigma)\sin(\gamma)}{R} & \frac{\sin(\sigma)}{R} & \sin(\gamma) & -\cos(\gamma) & 0 \\ \frac{\sin(\gamma)}{R\sin(\sigma)} & \frac{-\cos(\gamma)}{R\sin(\sigma)} & 0 & \frac{\cos(\gamma)\cos(\sigma)}{\sin(\sigma)} & \frac{\sin(\gamma)\cos(\sigma)}{\sin(\sigma)} & -1 \end{bmatrix} \quad (3)$$

desired image features have been achieved before the stopping criteria was met. This is shown in figure 7. On closer inspection, and considering the dynamics of a fixed wing aircraft, the control commands may not be achievable. The yaw rate is positive whilst the roll rate is negative. This would mean that although the pitch commands may be achieved, the aircraft would be asked to roll in one direction and yaw in the other. A better solution would ensure the roll and yaw rates are in the same direction, allowing for a coordinated turn. We notice however, that the yaw and pitch rate commands force the camera to descend and turn away from the target. The controller has assumed knowledge of range

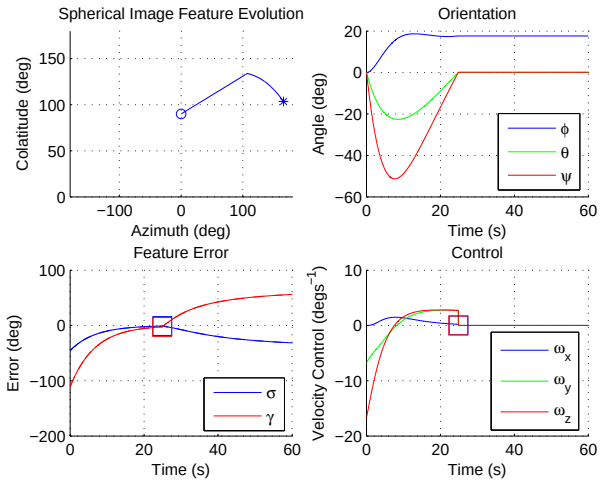

Fig. 7 Feature error, control & orientation for static case using Roll, Pitch and Yaw control.

to measure the optic flow from translational motion, $\frac{1}{R}\mathbf{L}_t$. This could be too small to measure accurately due to the $\frac{1}{R}$ term. This assumption is supported by recently reported performance limitations on angular measurements from EO sensors [28], past studies [17] [18] and figure 8. The optic flow from rotation is much larger than that from the translational velocities, so we could then consider a controller independent of range. This

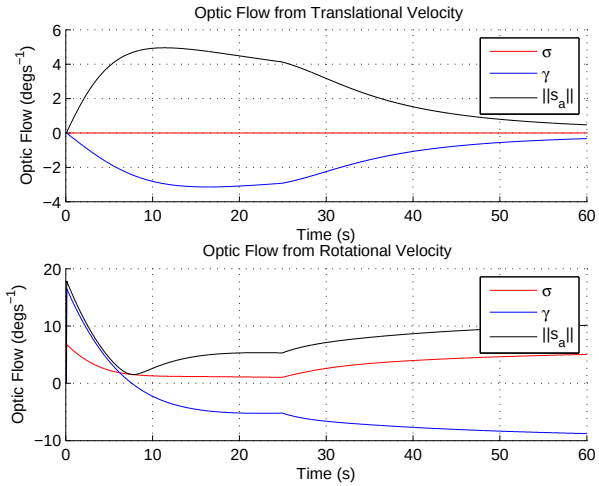

Fig. 8 Optic flow from translational and rotational degrees of freedom.

is given by

$$\omega = -\lambda \hat{\mathbf{L}}_{\omega}^{+} \tilde{\mathbf{e}} \quad (4)$$

where $\tilde{\mathbf{e}}$ is derived using the image features ($\tilde{\sigma}$ and $\tilde{\gamma}$) taken from the de-rotated image. We could then select the degree of freedom we wish to control according to which dimension we wish to avoid the target. This cannot guarantee the control will move the feature to the desired position in both azimuth and colatitude, but will move the target toward a safer region of the imaging sphere.

4 Aircraft Simulation

Based on the analysis of section 3, we conduct simulations for static and dynamic collision avoidance in the lateral and vertical directions separately. We implement the control architecture of figure 4 using a full non-linear model of a small Flamingo UAS for aircraft dynamics. Simulations are run over 80 seconds with the initial parameters and aircraft performance limitations defined in table 1. The visual controller gain is set to 0.15 and guidance is issued at 25Hz. Four separate PID loops are used for roll, heading, pitch and speed, running at 50Hz. The speed of both

Table 1 Simulation Parameters & Aircraft Limitations

Parameter	Static	Dynamic
Velocity (kts)	58	58
Target Velocity (kts)	0	80
Target Position (m)	[1000 0 -1000]	Variable
Max Roll (deg)	25	25
Max Pitch (deg)	12	12
$\mathbf{s}^*$ (deg)	[135 110]	[135 110]

target and own ship is held constant throughout the simulations whilst the autopilot configuration changes with guidance source. When guided using the visual control, the pitch and roll displacement autopilots are engaged, otherwise the pitch and heading displacement autopilots are used. The pitch rate and yaw rate commands are converted to pitch and roll angle commands using (5) and (6) respectively.

$$\theta^r(k) = \theta(k) + \omega_y^r(k)\Delta t \tag{5}$$

$$\phi^r(k) = \tan^{-1}\frac{V(k)\omega_z^r(k)}{g} \tag{6}$$

4.1 Static Target

In the static case, the target is not detected until less than 500m away and only lateral avoidance is used. Typically a static target would be attached to the ground or hanging, so the choice is justified. The target appears slightly above the aircraft and directly in front.

Figure 9 shows the trajectory of the aircraft avoiding the object by more than the required minimum separation. The feature error, control and aircraft orientation are depicted in figure 10. The commanded angles are depicted using a the subscript c. The commanded yaw, although not used directly, is also shown to verify the control in 6. The desired azimuth angle is just achieved before the stopping criteria is met. It is then allowed to change freely, as the conflict is considered resolved as far as the own ship is concerned. The colatitude angle has remained approximately constant, indicating a constant aircraft altitude.

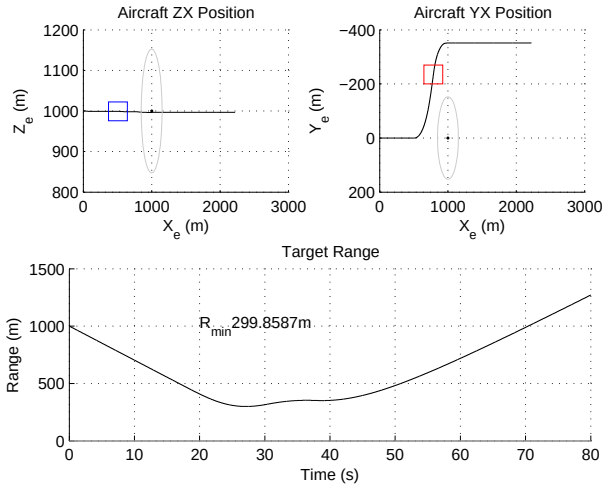

Fig. 9 Position & range to target for static case.

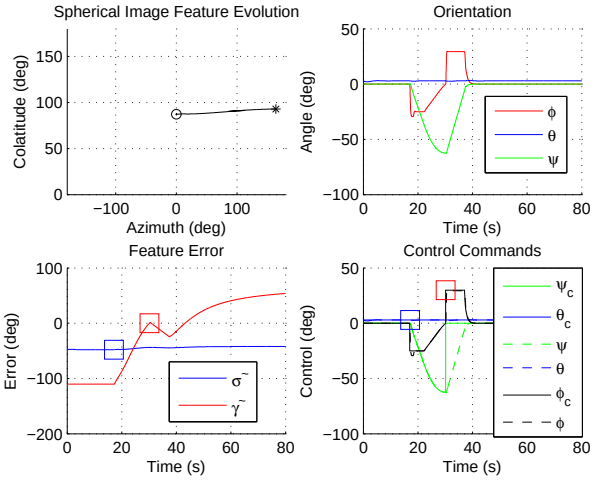

Fig. 10 Feature error, control & orientation for static case.

4.2 Dynamic Target

Strictly speaking the control for the dynamic case should be expressed by (7), where $\frac{\partial \varepsilon}{\partial t}$ is the motion of the target as projected onto the imaging sphere.

$$\hat{\omega} = \omega + \frac{\partial \varepsilon}{\partial t} \tag{7}$$

In a collision scenario, without action the point remains relatively stationary [13]. Section 3 showed that the optic flow from the translational

motion using a static target is relatively small, so looking at the problem in reverse, we can assume that the target motion on the image is also small. Considering the larger distances involved, this can be considered a valid assumption for initial control. For this reason we use the same controller for dynamic targets. Two cases are presented. In both cases the target approaches at an angle of 25° and constant 80kts velocity. Without action, a collision will occur at 5s after initial detection ($t_{cp} = 5$). This is a difficult case and under the expected average time to impact of 12s [13]. In the first case lateral avoidance is used and in the second vertical. The aircraft trajectories are shown in figures 11 and 12 respectively.

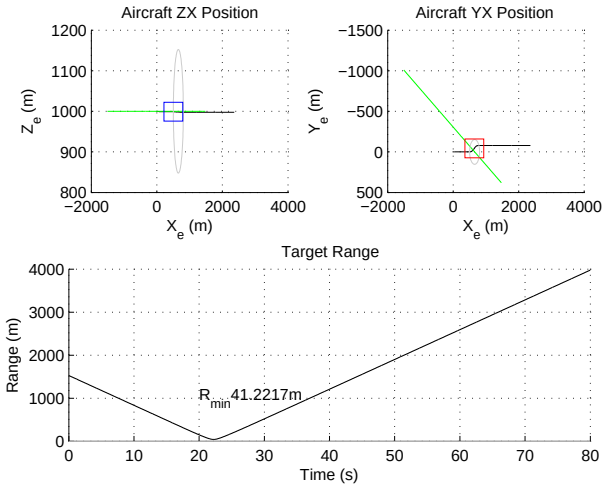

Fig. 11 Position & range to target for $t_{cp} = 5$ using lateral avoidance.

The aircraft was capable of avoiding the target in both cases, with increased miss distance in the lateral direction. The minimum safe separation distance was not achieved in either direction, however the result is still positive as it shows the approaches ability to react quickly to at least prevent impact.

The feature error, control and orientation are shown in figures 13 and 14 for each case. The desired image features were achieved just before the stopping criteria was met. In both cases the angles then diverge rapidly, settling at angles that correspond to a target that is behind and above the aircraft. This is because as the target approaches, the optic flow from the translational velocity becomes large and the previous assumptions are violated.

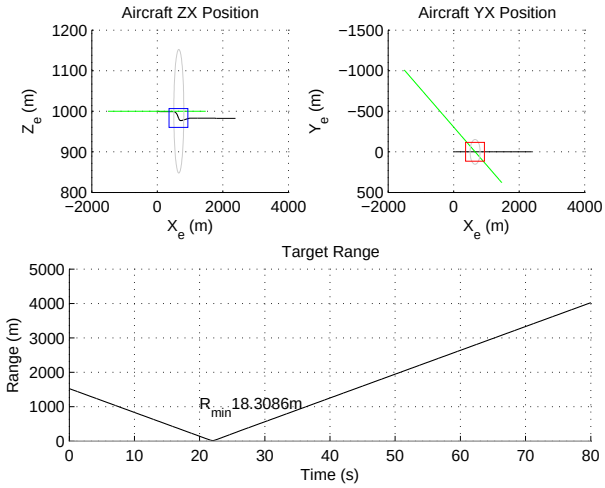

Fig. 12 Position & range to target for $t_{cp} = 5$ using vertical avoidance.

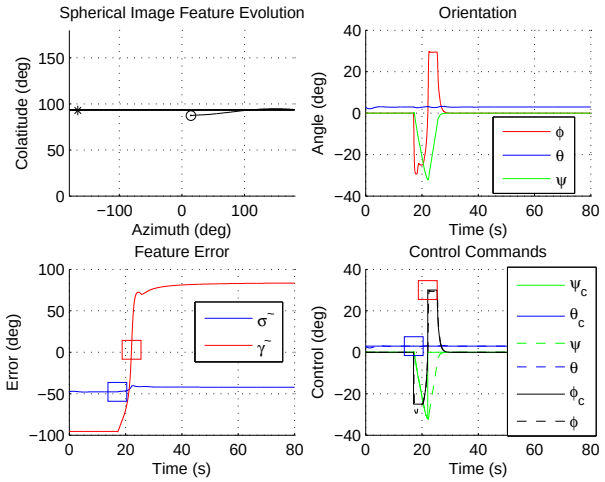

Fig. 13 Feature error, control & orientation for $t_{cp} = 5$ using lateral avoidance.

This is not a drawback from a collision avoidance point of view. Accounting for the translational velocity and using (2) would have forced the controller to issue weaker avoidance commands, reducing the separation distance in both lateral and vertical directions. The effect of inaccurate range estimates on collision avoidance performance is studied for a similar controller in [26] using a quad rotor platform.

In the last simulation we study a typical encounter scenario whereby the expected time until

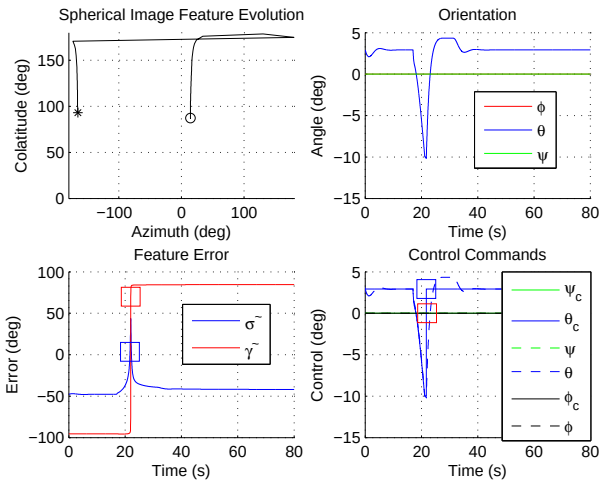

Fig. 14 Feature error, control & orientation for $t_{cp} = 5$ using vertical avoidance.

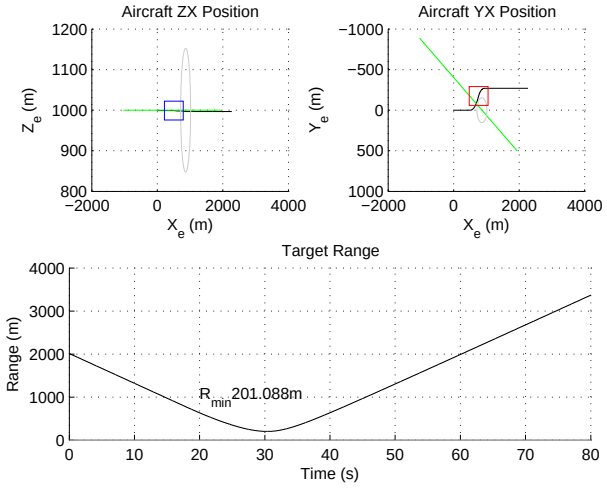

Fig. 15 Feature error, control & orientation for $t_{cp} = 12$ using lateral avoidance.

collision is 12 seconds and the target is approaching head on at 80kts. We use lateral avoidance based on previous results. Figure 15 shows the trajectory. The aircraft was able to avoid the target by more than the required minimum separation, therefore successfully avoiding a near mid air collision (NMAC).

We could have converted the pitch command into an altitude reference command and used an altitude hold autopilot instead. If we consider that we are moving with inertial velocity V, we can approximate the z velocity resulting from that pitch value. This can be integrated over one time step and added to the current altitude. When implemented however, the aircraft displayed oscillatory motion in the vertical plane as it avoided the target, attempting to level off after each command. This is not ideal and with an excess of control effort. The autopilot could be tuned to provide better performance, but we would expect similar results for vertical avoidance.

Only selecting one degree of freedom to use for control cannot guarantee achieving the desired features. This would not be the case if all 3 angular rates were controlled. Aircraft limitations force us to use only one or two. Deriving a controller explicitly for yaw and pitch, having accounted for the roll, may be a better approach to allow for avoidance in two directions simultaneously. This would provide increased miss distance and ensure the features converge to the desired position. It was observed that attempting to hold constant angles in the image is difficult, due to the velocities at which aircraft operate at. For this reason it may be better to consider servoing to a region of the sphere instead, which would also allow us to use less control effort in some cases.

5 Conclusion

A general guidance and control scheme for a vision based automated Sense and Avoid system was presented. A spherical camera model is used to ensure target visibility is maintained throughout the encounter whilst image-based visual servoing techniques were used for control. The approach provides lateral or vertical separation without requiring a range estimate, and a simple stopping criteria is used to terminate the avoidance commands. Simulation studies have verified the controllers ability to avoid collision of static and constant velocity targets. More simulation studies on a diverse range of encounter scenarios would be required to ensure the robustness of the approach.

Further work includes deriving a visual controller explicitly for 2DOF, as opposed to 3DOF, and studying the effects of camera orientation on the derived control scheme. Additionally, visual

servoing techniques that do not need to select a desired position, but instead use a region based approach, would be better suited to this problem.

References

[1] Dalamagkidis, K. and Valavanis, K. P. and Piegl, L. A. "On unmanned aircraft systems issues, challenges and operational restrictions preventing integration into the National Airspace System," *Progress in Aerospace Sciences*, vol. 44, pp. 503–519, Nov. 2008.

[2] Barfield, F. and Res, W. and Center, D. and Wright-Patterson, A. F. B. "Autonomous collision avoidance: the technical requirements," *Proceedings of the IEEE 2000 National Aerospace and Electronics Conference (NAECON)*, Oct. 2000.

[3] Geyer, C. and Singh, S. and Chamberlain, L. "Avoiding collisions between aircraft: state of the art and requirements for UAVs operating in civilian airspace," *Technical Report: CMU-RI-TR-08-03*, March 2008.

[4] Kephart, R. J. "Comparison of See-and-Avoid performance in manned and remotely piloted aircraft," *PhD dissertation*, Ohio University, Nov. 2008.

[5] Lai, J. and Mejias, L and Ford, J.J. "Airborne vision-based collision-detection system," *Journal of Field Robotics*, vol. 28, pp. 137–157, March 2011.

[6] Mejias, L. and Ford, J. and Lai, J. S. "Towards the implementation of vision-based UAS sense-and-avoid," *Proceedings of the 27th International Congress of the Aeronautical Sciences (ICAS)*, Sep. 2010.

[7] Gandhi, T. and Yang, M. and Kasturi, R. and Camps, and O. Coraor, L. and McCandless. J. "Detection of obstacles in flight path of an aircraft," *IEEE Transactions on Aerospace and Electronic Systems*, vol. 39, pp. 176–191, Jan. 2003.

[8] Maddern, W. and Wyeth, G. "Development of a hemispherical compound eye for egomotion estimation," *Proceedings of the 2008 Australasian Conference on Robotics & Automation (ACRA)*, Dec. 2008.

[9] Gurunandan, K. and Hayar, S. "Towards a true spherical camera," *Proceedings of Human Vision and Electronic Imaging XIV (SPIE)*, Jan. 2009.

[10] Geyer, C. and Daniilidis, K. "A unifying theory for central panoramic systems and practical implications," *Proceedings of the 6th European Conference on Computer Vision (ECCV)*, June. 2000.

[11] Wainwright, A and Ford, J. J and Lai, J. S. "Fat and thin adaptive HMM filters for vision based detection of moving targets," *Proceedings of the 2011 Australasian Conference on Robotics & Automation (ACRA)*, Dec. 2011.

[12] Kuchar, J. and Yang, L. C. "Survey of conflict detection and resolution modeling methods," *IEEE Transactions on Intelligent Transportation Systems*, vol. 1, pp. 179–189, Dec. 2000.

[13] Australian Transport Safety Bureau (ATSB) "Limitations of the See-and-Avoid principle," Australian Government, 2004.

[14] Morris, C. C. "Midair collisions: limitations of the see-and-avoid concept in civil aviation," *Aviation, Space, and Environmental Medicine*, vol. 76, pp. 357–365, 2005.

[15] Grilley, D. E. "Resolution requirements for passive Sense & Avoid," *Proceedings of AUVSI Conference*, June 2005

[16] Angelov, P. and Bocaniala, C. D. and Xydeas, C. and Pattchett, C. and Ansell, D. and Everett, M. and Leng, G. "A passive approach to autonomous collision detection and avoidance in uninhabited aerial systems," *Proceedings of the 10th International Conference on Computer Modeling and Simulation*, Sep. 2008.

[17] Kochenderfer, M. J. and Griffith, J. D. and Kuchar, J. K. "Hazard alerting using line-of-sight rate," *Proceedings of the AIAA Guidance, Navigation and Control Conference and Exhibit*, Aug. 2008.

[18] Shakernia, O. and Chen, W. Z. and Graham, S. and Zvanya, J. and White, A. and Weingarten, N. and Raska, V. M. "Sense and Avoid (SAA) flight test and lessons learned," *Proceedings of the AIAA Infotech@Aerospace 2007 Conference and Exhibit*, May 2007.

[19] Bourquardez, O. and Chaumette, F. "Visual servoing of an airplane for auto-landing," *Proceedings of the IEEE/RSJ 2007 International Conference on Intelligent Robots and Systems (IROS)*,

Oct. 2007.

[20] Hutchinson, S. and Hager, G. D. and Corke, P. I. "A tutorial on visual servo control," *IEEE Transactions on Robotics and Automation*, vol. 12, pp. 651–670, Oct. 1996.

[21] Beyeler, A. and Zufferey, J. and Floreano, D. "Vision-based control of near-obstacle flight," *Autonomous Robots*, vol 27, pp. 201–219, July 2009.

[22] Zufferey, J.-C. and Floreano, D. "Toward 30-gram autonomous indoor aircraft: vision-based obstacle avoidance and altitude control," *Proceedings of the IEEE 2009 International Conference on Robotics and Automation (ICRA)*, May 2009.

[23] Sharma, R. and Saunders, J. and Beard, R. "Reactive path planning for micro air vehicles using bearing only measurements," *Journal of Intelligent & Robotic Systems*, vol. 65, pp. 409–416, Jan. 2012.

[24] Saunders, J. and Beard, R. and Byrne, J. "Vision-based reactive multiple obstacle avoidance for micro air vehicles," *Proceedings of the 2009 American Control Conference (ACC)*, June 2009.

[25] Boyadzhiev, K. N. "Spirals and conchospirals in flight of insects," *The College Mathematics Journal*, vol. 30, pp. 23–31, Jan. 1999.

[26] Mcfadyen, A. D and Corke, P. and Mejias, L "Rotorcraft collision avoidance using spherical image based visual servoing and single point features," *Proceedings of the IEEE/RSJ 2012 Conference on Intelligent Robotics & Systems (IROS)*, Oct. 2012 *(Accepted)*

[27] Federal Aviation Regulation (FAA). *Sec.91.113: Right-of-Way Rules*

[28] Bruggemann, T. and Mejias, L. "Accuracy of monocular vision-derived angles to a threat for see and avoid control," *Proceedings of the 28th International Congress of the Aeronautical Sciences (ICAS)*, Sep. 2012. *(Accepted)*

[29] Corke, P. I. "Spherical image-based visual servo and structure estimation," *Proceedings of the IEEE 2010 International Conference on Robotics and Automation (ICRA)*, May 2010.

[30] Corke, P. I. and Spindler, F. and Chaumette, F. "Combining cartesian and polar coordinates in IBVS," *Proceedings of the IEEE/RSJ 2009 International Conference on Intelligent Robots and Systems (IROS)*, Oct. 2009.

5.1 Copyright Statement